


Cite this: *RSC Adv.*, 2021, 11, 1736

# Effect of Ni/Co mass ratio and NiO–Co<sub>3</sub>O<sub>4</sub> loading on catalytic performance of NiO–Co<sub>3</sub>O<sub>4</sub>/Nb<sub>2</sub>O<sub>5</sub>–TiO<sub>2</sub> for direct synthesis of 2-propylheptanol from *n*-valeraldehyde†

Lili Zhao,<sup>ab</sup> Hualiang An,<sup>\*a</sup> Xinqiang Zhao<sup>ID</sup> <sup>\*a</sup> and Yanji Wang<sup>ID</sup> <sup>a</sup>

In the direct synthesis of 2-propylheptanol (2-PH) from *n*-valeraldehyde, a second-metal oxide component Co<sub>3</sub>O<sub>4</sub> was introduced into NiO/Nb<sub>2</sub>O<sub>5</sub>–TiO<sub>2</sub> catalyst to assist in the reduction of NiO. In order to optimize the catalytic performance of NiO–Co<sub>3</sub>O<sub>4</sub>/Nb<sub>2</sub>O<sub>5</sub>–TiO<sub>2</sub> catalyst, the effects of the Ni/Co mass ratio and NiO–Co<sub>3</sub>O<sub>4</sub> loading were investigated. A series of NiO–Co<sub>3</sub>O<sub>4</sub>/Nb<sub>2</sub>O<sub>5</sub>–TiO<sub>2</sub> catalysts with different Ni/Co mass ratios were prepared by the co-precipitation method and their catalytic performances were evaluated. The result showed that NiO–Co<sub>3</sub>O<sub>4</sub>/Nb<sub>2</sub>O<sub>5</sub>–TiO<sub>2</sub> with a Ni/Co mass ratio of 8/3 demonstrated the best catalytic performance because the number of d-band holes in this catalyst was nearly equal to the number of electrons transferred in hydrogenation reaction. Subsequently, the NiO–Co<sub>3</sub>O<sub>4</sub>/Nb<sub>2</sub>O<sub>5</sub>–TiO<sub>2</sub> catalysts with different Ni/Co mass ratios were characterized by XRD and XPS and the results indicated that both an interaction of Ni with Co and formation of a Ni–Co alloy were the main reasons for the reduction of NiO–Co<sub>3</sub>O<sub>4</sub>/Nb<sub>2</sub>O<sub>5</sub>–TiO<sub>2</sub> catalyst in the reaction process. A higher NiO–Co<sub>3</sub>O<sub>4</sub> loading could increase the catalytic activity but too high a loading resulted in incomplete reduction of NiO–Co<sub>3</sub>O<sub>4</sub> in the reaction process. Thus the NiO–Co<sub>3</sub>O<sub>4</sub>/Nb<sub>2</sub>O<sub>5</sub>–TiO<sub>2</sub> catalyst with a Ni/Co mass ratio of 8/3 and a NiO–Co<sub>3</sub>O<sub>4</sub> loading of 14 wt% showed the best catalytic performance; a 2-PH selectivity of 80.4% was achieved with complete conversion of *n*-valeraldehyde. Furthermore, the NiO–Co<sub>3</sub>O<sub>4</sub>/Nb<sub>2</sub>O<sub>5</sub>–TiO<sub>2</sub> catalyst showed good stability. This was ascribed to the interaction of Ni with Co, the formation of the Ni–Co alloy and further reservation of both in the process of reuse.

Received 19th October 2020  
Accepted 22nd December 2020

DOI: 10.1039/d0ra08903f

rsc.li/rsc-advances

## 1. Introduction

As an environmentally friendly plasticizer alcohol, 2-propylheptanol (2-PH) can replace 2-ethylhexanol in the production of plasticizers. The industrial process for production of 2-PH comprises a liquid-phase self-condensation of *n*-valeraldehyde and a subsequent gas-phase hydrogenation of 2-propyl-2-heptenal. The liquid-phase self-condensation of *n*-valeraldehyde utilizing a dilute NaOH solution as catalyst suffers from several drawbacks such as environmental pollution, apparatus corrosion, and difficulty in recovering and recycling catalyst. The gas-phase hydrogenation of 2-propyl-2-heptenal requires a high energy consumption. If *n*-valeraldehyde self-

condensation and 2-propyl-2-heptenal hydrogenation can be integrated using a multifunctional solid catalyst, that is, direct synthesis of 2-PH from *n*-valeraldehyde, the industrial production of 2-PH can not only simplify the flow process, but also conform to the requirements for green and sustainable development. Therefore, the multifunctional solid catalyst with high catalytic performance is very important for the reaction integration.

At present, the direct synthesis of 2-PH from *n*-valeraldehyde was reported over Ru-HT (ruthenium hydrotalcite) bifunctional catalyst but the selectivity of 2-PH was only 48%.<sup>1</sup> In a similar reaction integration system, Ni/Ce–Al<sub>2</sub>O<sub>3</sub> showed a better catalytic performance for direct synthesis of 2-ethylhexanol from *n*-butanal.<sup>2</sup> However, the selectivity of 2-ethylhexanol was only 66.9% with a 100% of *n*-butanal conversion. Additionally, the catalyst suffered from the problem of deactivation due to hydration of  $\gamma$ -Al<sub>2</sub>O<sub>3</sub>. It is obvious that improvement of both target product selectivity and catalyst stability is still an unsolved problem.

Titanium dioxide is not only a well-known photocatalyst,<sup>3,4</sup> but also can be a good heterogeneous catalyst in the replacement of microporous zeolites and mesoporous (M41S, SBA)

<sup>a</sup>Hebei Provincial Key Lab of Green Chemical Technology and High Efficient Energy Saving, Hebei University of Technology, Tianjin 300130, China. E-mail: zhaoxq@hebut.edu.cn; anhl@hebut.edu.cn

<sup>b</sup>College of Science and Technology, Hebei Agricultural University, Huanghua, Hebei 061100, China

† Electronic supplementary information (ESI) available: XPS spectra of NiO–Co<sub>3</sub>O<sub>4</sub>/Nb<sub>2</sub>O<sub>5</sub>–TiO<sub>2</sub> with different Ni/Co mass ratios before and after reaction; catalytic performance of NiO–Co<sub>3</sub>O<sub>4</sub>/Nb<sub>2</sub>O<sub>5</sub>–TiO<sub>2</sub>. See DOI: 10.1039/d0ra08903f



materials.<sup>5</sup> The KIT-6 incorporating transition metals (Al, Ti, Ce) catalysts with various catalytic applications have high hydrothermal stability compared with the M41S and SBA-15 materials.<sup>5–7</sup> In addition, in our previous study on the *n*-valeraldehyde self-condensation,<sup>8</sup> TiO<sub>2</sub> showed a high catalytic performance and exhibited a good stability. Moreover, we also evaluated the catalytic performance of Ni/TiO<sub>2</sub> for liquid-phase hydrogenation of 2-propyl-2-heptenal and found that Ni/TiO<sub>2</sub> had a fairly high hydrogenation performance.<sup>9</sup> Based on the above results, we first implemented the one-step synthesis of 2-PH from *n*-valeraldehyde over Ni/TiO<sub>2</sub> catalyst and found that the selectivity of 2-PH was very poor due to a lower competitiveness of *n*-valeraldehyde self-condensation to *n*-valeraldehyde hydrogenation. In order to improve the catalytic performance of Ni/TiO<sub>2</sub> for *n*-valeraldehyde self-condensation, Ni/TiO<sub>2</sub> was modified by Nb<sub>2</sub>O<sub>5</sub> to tune its acidity and basicity. Therefore, Nb<sub>2</sub>O<sub>5</sub>-TiO<sub>2</sub> mainly play a catalytic role in the *n*-valeraldehyde self-condensation. Then the catalytic performance of NiO/Nb<sub>2</sub>O<sub>5</sub>-TiO<sub>2</sub> catalyst was investigated in order to delay the formation of metal sites on the catalyst surface for further improving the competitiveness of *n*-valeraldehyde self-condensation reaction. However, NiO was not completely reduced in reaction. To facilitate the complete reduction of NiO in reaction, MO<sub>x</sub> (M = Pd, Co, Ir or Rh) was introduced into NiO/Nb<sub>2</sub>O<sub>5</sub>-TiO<sub>2</sub> catalyst to lower the reduction temperature of NiO.<sup>10</sup>

The key to promotion of 2-PH selectivity in this reaction integration is to enhance competitiveness of *n*-valeraldehyde self-condensation with respect to direct hydrogenation since the two parallel reactions exist in this reaction system. For this purpose, NiO-Co<sub>3</sub>O<sub>4</sub>/Nb<sub>2</sub>O<sub>5</sub>-TiO<sub>2</sub> was utilized to catalyze the direct synthesis of 2-PH from *n*-valeraldehyde by means of a reduction-in-reaction operation (reduction of NiO-Co<sub>3</sub>O<sub>4</sub> and *n*-valeraldehyde self-condensation proceeded simultaneously) in our previous work.<sup>9</sup> Therefore, NiO-Co<sub>3</sub>O<sub>4</sub> can be reduced to Ni-Co in the stage of *n*-valeraldehyde self-condensation reaction, which would play an important role in the successive hydrogenation of self-condensation product or *n*-valeraldehyde. In this way, *n*-valeraldehyde self-condensation reaction showed a competitive advantage over its direct hydrogenation since the appearance of metal sites (Ni-Co) was delayed. Therefore selectivity of 2-PH was enhanced while that of *n*-pentanol was depressed. To further improve the catalytic performance of NiO-Co<sub>3</sub>O<sub>4</sub>/Nb<sub>2</sub>O<sub>5</sub>-TiO<sub>2</sub>, effects of Ni/Co mass ratio and NiO-Co<sub>3</sub>O<sub>4</sub> loading were investigated in this work. On this basis, a superior catalytic performance of NiO-Co<sub>3</sub>O<sub>4</sub>/Nb<sub>2</sub>O<sub>5</sub>-TiO<sub>2</sub> was achieved and the reason for its good reusability was analyzed.

## 2. Experimental

### 2.1 Catalyst preparation

TiO<sub>2</sub> was prepared by a sol-gel method according to the literature<sup>8</sup> and Nb<sub>2</sub>O<sub>5</sub>-TiO<sub>2</sub> was prepared by impregnating TiO<sub>2</sub> with an aqueous solution of niobic acid (niobium hydroxide) (dissolving 0.278 g niobic acid (niobium hydroxide) in 50 mL oxalic acid solution (0.5 mol L<sup>-1</sup>)), followed by aged at room

temperature for 12 h, evaporated at 70 °C for 5 h, dried at 120 °C for 12 h and calcination of 450 °C for 2 h.

NiO-Co<sub>3</sub>O<sub>4</sub>/Nb<sub>2</sub>O<sub>5</sub>-TiO<sub>2</sub> catalyst was prepared by co-impregnating Nb<sub>2</sub>O<sub>5</sub>-TiO<sub>2</sub> with an aqueous solution of Ni(NO<sub>3</sub>)<sub>2</sub>·6H<sub>2</sub>O and Co(NO<sub>3</sub>)<sub>2</sub>·6H<sub>2</sub>O (2.478 g of Ni(NO<sub>3</sub>)<sub>2</sub>·6H<sub>2</sub>O and 0.247 g of Co(NO<sub>3</sub>)<sub>2</sub>·6H<sub>2</sub>O were separately dissolved in 50 mL distilled water), followed by aged at room temperature for 12 h, evaporated at 70 °C for 5 h, dried at 100 °C for 12 h and calcination of 450 °C for 2 h.

NiO/Nb<sub>2</sub>O<sub>5</sub>-TiO<sub>2</sub> or Co<sub>3</sub>O<sub>4</sub>/Nb<sub>2</sub>O<sub>5</sub>-TiO<sub>2</sub> catalyst was prepared by impregnating Nb<sub>2</sub>O<sub>5</sub>-TiO<sub>2</sub> with an aqueous solution of Ni(NO<sub>3</sub>)<sub>2</sub>·6H<sub>2</sub>O or Co(NO<sub>3</sub>)<sub>2</sub>·6H<sub>2</sub>O and the remaining steps were similar to the preparation of NiO-Co<sub>3</sub>O<sub>4</sub>/Nb<sub>2</sub>O<sub>5</sub>-TiO<sub>2</sub> catalyst.

### 2.2 Catalyst characterization

X-ray diffraction (XRD) patterns were measured on a Bruker D8 Advance X-ray diffractometer equipped with a Cu K $\alpha$  radiation and a graphite monochromator at 100 mA and 40 kV. The scan range covered from 10° to 90° at a rate of 4° min<sup>-1</sup>.

X-ray photoelectron spectroscopy (XPS) analysis were conducted on a Physical Electronics Kratos Axis Ultra DLD using monochromatic Al K $\alpha$  X-rays (1486.6 eV) operated at 150 W and 15 kV. The narrow-spectra were obtained with a pass energy of 40 eV and a step increment of 0.100 eV. C 1s peak of 284.6 eV was used as a calibration standard to calibrate the binding energy values.

### 2.3 Catalyst activity evaluation

30 mL (24 g) of *n*-valeraldehyde and 3.6 g of NiO-Co<sub>3</sub>O<sub>4</sub>/Nb<sub>2</sub>O<sub>5</sub>-TiO<sub>2</sub> catalyst were placed in a 100 mL stainless steel autoclave and then the air inside was replaced with hydrogen. The mixture was heated to 200 °C and kept for 6 h under a H<sub>2</sub> pressure of 3.0 MPa while stirring. After the completion of reaction, the mixture was cooled to room temperature and was separated by centrifugation, and then the liquid was quantitatively analyzed on a SP-2100 gas chromatograph (Beijing Beifen-Ruili Analytical Instrument Co., Ltd) equipped with a flame ionization detector (FID) and a KB-1 capillary column. Cyclohexanol was used as internal standard for improving analytical accuracy.

## 3. Results and discussion

### 3.1 Effect of Ni/Co mass ratio

The effect of Ni/Co mass ratio on the catalytic performance of NiO-Co<sub>3</sub>O<sub>4</sub>/Nb<sub>2</sub>O<sub>5</sub>-TiO<sub>2</sub> was investigated and the results are shown in Table 1. It can be seen that all NiO-Co<sub>3</sub>O<sub>4</sub>/Nb<sub>2</sub>O<sub>5</sub>-TiO<sub>2</sub> catalysts showed better performance than NiO/Nb<sub>2</sub>O<sub>5</sub>-TiO<sub>2</sub> or Co<sub>3</sub>O<sub>4</sub>/Nb<sub>2</sub>O<sub>5</sub>-TiO<sub>2</sub> catalyst. More specifically, the condensation product was not completely hydrogenated over NiO/Nb<sub>2</sub>O<sub>5</sub>-TiO<sub>2</sub> or Co<sub>3</sub>O<sub>4</sub>/Nb<sub>2</sub>O<sub>5</sub>-TiO<sub>2</sub> catalyst, indicating that a lower hydrogenation activity was ascribed to incomplete reduction of NiO or Co<sub>3</sub>O<sub>4</sub> in the reaction process. However, 2-PH was formed as the main product over NiO-Co<sub>3</sub>O<sub>4</sub>/Nb<sub>2</sub>O<sub>5</sub>-TiO<sub>2</sub> catalysts with different Ni/Co mass ratios. With a decrease of Ni/Co mass



Table 1 Effect of Ni/Co mass ratio on catalytic performance of NiO–Co<sub>3</sub>O<sub>4</sub>/Nb<sub>2</sub>O<sub>5</sub>–TiO<sub>2</sub> catalyst<sup>a</sup>

Catalyst	Ni/Co mass ratio	X <sub>V</sub> /%	S <sub>PO</sub> /%	S <sub>2-PHEA</sub> /%	S <sub>2-PHA</sub> /%	S <sub>2-PH</sub> /%
NiO/Nb <sub>2</sub> O <sub>5</sub> –TiO <sub>2</sub> <sup>b</sup>	—	93.1	3.2	56.0	39.6	0
NiO–Co <sub>3</sub> O <sub>4</sub> /Nb <sub>2</sub> O <sub>5</sub> –TiO <sub>2</sub>	10	100	21.8	0	0	77.1
NiO–Co <sub>3</sub> O <sub>4</sub> /Nb <sub>2</sub> O <sub>5</sub> –TiO <sub>2</sub>	8/3	100	18.2	0	0	81.4
NiO–Co <sub>3</sub> O <sub>4</sub> /Nb <sub>2</sub> O <sub>5</sub> –TiO <sub>2</sub>	6/5	100	34.1	0	0	59.3
NiO–Co <sub>3</sub> O <sub>4</sub> /Nb <sub>2</sub> O <sub>5</sub> –TiO <sub>2</sub>	4/7	100	36.7	0	0	56.3
Co <sub>3</sub> O <sub>4</sub> /Nb <sub>2</sub> O <sub>5</sub> –TiO <sub>2</sub>	—	100	20.6	23.1	24.1	13.0

<sup>a</sup> Reaction conditions: a weight percentage of catalyst = 15%,  $T = 200\text{ }^{\circ}\text{C}$ ,  $P = 3\text{ MPa}$ ,  $t = 6\text{ h}$ . X: conversion; S: selectivity. V: *n*-valeraldehyde; PO: *n*-pentanol; 2-PHEA: 2-propyl-2-heptenal; 2-PHA: 2-propylheptanal; 2-PH: 2-propylheptanol. <sup>b</sup> The yield of *n*-pentanol, 2-propyl-2-heptenal, 2-propylheptanal and 2-propylheptanol was respectively 3.0%, 52.1%, 36.9% and 0%.

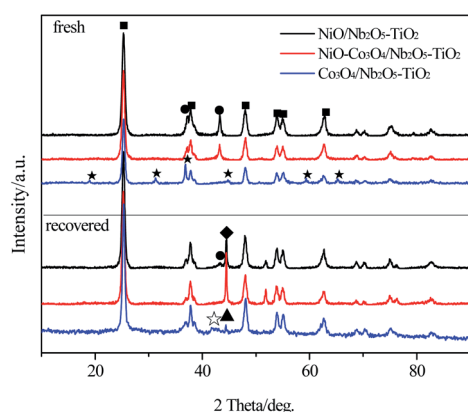


Fig. 1 XRD patterns of NiO/Nb<sub>2</sub>O<sub>5</sub>–TiO<sub>2</sub>, Co<sub>3</sub>O<sub>4</sub>/Nb<sub>2</sub>O<sub>5</sub>–TiO<sub>2</sub> and NiO–Co<sub>3</sub>O<sub>4</sub>/Nb<sub>2</sub>O<sub>5</sub>–TiO<sub>2</sub> with a Ni/Co mass ratio of 8/3 before and after reaction. ■: TiO<sub>2</sub>; ◆: NiO; ★: Co<sub>3</sub>O<sub>4</sub>; ▲: NiO; ▲: CoO; ☆: CoO.

ratio, selectivity of 2-PH increased slightly firstly, attained its highest value (81.4%) at a Ni/Co mass ratio of 8/3 and then dropped while that of *n*-pentanol changed just the opposite.

XRD patterns of the fresh and the recovered catalysts of NiO/Nb<sub>2</sub>O<sub>5</sub>–TiO<sub>2</sub>, Co<sub>3</sub>O<sub>4</sub>/Nb<sub>2</sub>O<sub>5</sub>–TiO<sub>2</sub> and NiO–Co<sub>3</sub>O<sub>4</sub>/Nb<sub>2</sub>O<sub>5</sub>–TiO<sub>2</sub> with a Ni/Co mass ratio of 8/3 are shown in Fig. 1. TiO<sub>2</sub> anatase crystallite phases were clearly observed in all catalyst samples. The diffraction peaks at  $2\theta$  of 37.3° and 43.3° in the fresh NiO/Nb<sub>2</sub>O<sub>5</sub>–TiO<sub>2</sub> were attributed to (111) and (200) crystal planes of

NiO respectively. Similarly, six peaks at  $2\theta$  of 19.0°, 31.3°, 36.9°, 44.8°, 59.4° and 65.3° was respectively ascribed to (111), (220), (311), (400), (511) and (440) crystal planes of Co<sub>3</sub>O<sub>4</sub> in the fresh Co<sub>3</sub>O<sub>4</sub>/Nb<sub>2</sub>O<sub>5</sub>–TiO<sub>2</sub>.<sup>11</sup> Whereas, the peaks of NiO were detected but that of Co<sub>3</sub>O<sub>4</sub> was not found due to a lower Co<sub>3</sub>O<sub>4</sub> loading, a smaller grain size and a higher dispersion on the supporter surface in the fresh NiO–Co<sub>3</sub>O<sub>4</sub>/Nb<sub>2</sub>O<sub>5</sub>–TiO<sub>2</sub> catalyst. For both the recovered NiO/Nb<sub>2</sub>O<sub>5</sub>–TiO<sub>2</sub> and Co<sub>3</sub>O<sub>4</sub>/Nb<sub>2</sub>O<sub>5</sub>–TiO<sub>2</sub> catalysts, it was obvious that the peaks of NiO or CoO were detected besides metallic Ni or Co, indicating that NiO or Co<sub>3</sub>O<sub>4</sub> was incompletely reduced in the reaction process. However, the peaks of NiO disappeared from the recovered NiO–Co<sub>3</sub>O<sub>4</sub>/Nb<sub>2</sub>O<sub>5</sub>–TiO<sub>2</sub>, indicating a complete reduction of NiO in the reaction process possibly due to an interaction of Ni with Co. This may explain the differences in the catalytic performance of the bimetallic oxides and monometallic oxides catalysts as showed in Table 1.

In order to further analyze the effect of an interaction of Ni with Co on the catalytic performance of NiO–Co<sub>3</sub>O<sub>4</sub>/Nb<sub>2</sub>O<sub>5</sub>–TiO<sub>2</sub>, the recovered NiO–Co<sub>3</sub>O<sub>4</sub>/Nb<sub>2</sub>O<sub>5</sub>–TiO<sub>2</sub> catalysts with different Ni/Co mass ratios were analyzed by XRD and the result is shown in Fig. 2. The characteristic peaks of anatase TiO<sub>2</sub> were clearly observed. However, the peaks of NiO and Co<sub>3</sub>O<sub>4</sub> were not detected in all catalyst samples.  $2\theta$  value of the corresponding (111) crystal facet was located at between 44.369° of pure metal Co (111) and 44.507° of pure metal Ni (111), indicating that Ni–Co alloy phase was formed during the reaction process.<sup>12</sup>

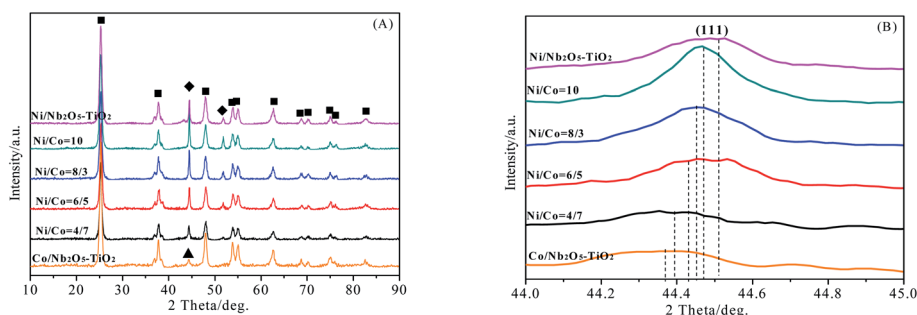


Fig. 2 XRD patterns of the recovered NiO–Co<sub>3</sub>O<sub>4</sub>/Nb<sub>2</sub>O<sub>5</sub>–TiO<sub>2</sub> catalyst with different Ni/Co mass ratios. ■: TiO<sub>2</sub>; ◆: NiO; ▲: CoO. (A) XRD patterns; (B) enlarged view of XRD patterns.



**Table 2** Ni 2p and Co 2p XPS data of the fresh NiO–Co<sub>3</sub>O<sub>4</sub>/Nb<sub>2</sub>O<sub>5</sub>–TiO<sub>2</sub> with different Ni/Co mass ratios

Ni/Co	Binding energy/eV					
	Ni <sup>2+</sup>		Co <sup>2+</sup>		Co <sup>3+</sup>	
	Ni 2p <sub>3/2</sub>	Ni 2p <sub>1/2</sub>	Co 2p <sub>3/2</sub>	Co 2p <sub>1/2</sub>	Co 2p <sub>3/2</sub>	Co 2p <sub>1/2</sub>
10	853.6	861.6	781.9	797.0	780.4	795.0
	855.4	872.8				
8/3	853.6	860.7	781.2	796.6	779.8	794.8
	855.5	872.5				
6/5	853.7	861.2	781.1	796.5	779.3	795.8
	855.6	872.7				
4/7	853.8	861.0	781.1	796.5	779.2	794.1
	855.5	873.0				

Moreover, the diffraction peak of Ni–Co alloy phase (111) crystal plane moved towards the direction of metal Co and gradually approached the characteristic peak of pure metal Co with a decrease of Ni/Co mass ratio. On the contrary, the diffraction peak of Ni–Co alloy phase (111) crystal plane moved towards the direction of metal Ni and gradually approached the characteristic peak of pure metal Ni with an increase of Ni/Co mass ratio.

The fresh and the recovered catalysts with different Ni/Co mass ratios were analyzed by means of XPS technique. The Ni 2p and Co 2p XPS spectra are shown in Fig. S1 in the ESI,† while the measurement data are listed in Tables 2 and 3. Table 2 listed Ni 2p and Co 2p binding energy in the fresh NiO–Co<sub>3</sub>O<sub>4</sub>/Nb<sub>2</sub>O<sub>5</sub>–TiO<sub>2</sub> catalysts with different Ni/Co mass ratios. According to the literatures,<sup>13,14</sup> the binding energies at 853.6–853.8 eV and 855.4–855.6 eV are attributed to Ni 2p<sub>3/2</sub> peaks of Ni<sup>2+</sup>, the binding energies at 860.7–861.6 eV and 872.5–873.0 eV are attributed to Ni 2p<sub>1/2</sub> peaks of Ni<sup>2+</sup>, the binding energies at 781.1–781.9 eV and 796.5–797.0 eV are separately attributed to Co 2p<sub>3/2</sub> and Co 2p<sub>1/2</sub> peaks of Co<sup>2+</sup>, the binding energies at 779.2–780.4 eV and 794.1–795.8 eV are respectively attributed to Co 2p<sub>3/2</sub> and Co 2p<sub>1/2</sub> peaks of Co<sup>3+</sup>. The above results indicate that the mixed metal oxides in the fresh catalyst are NiO and Co<sub>3</sub>O<sub>4</sub>. It can be seen from Table 3 that the binding energy at 852.0–852.2 eV is attributed to Ni 2p<sub>3/2</sub> peak of Ni<sup>0</sup> and the

binding energy at 778.1–778.3 eV is attributed to Co 2p<sub>3/2</sub> peak of Co<sup>0</sup> in the recovered NiO–Co<sub>3</sub>O<sub>4</sub>/Nb<sub>2</sub>O<sub>5</sub>–TiO<sub>2</sub> catalysts.<sup>15,16</sup> In addition, the characteristic peaks of NiO and CoO were also be detected due to reoxidation of metallic Ni and Co by contacting air in the analysis process. Moreover, the binding energy of Ni 2p<sub>3/2</sub> of Ni<sup>0</sup> in the recovered NiO–Co<sub>3</sub>O<sub>4</sub>/Nb<sub>2</sub>O<sub>5</sub>–TiO<sub>2</sub> is lower than that of pure Ni (852.4 eV) while the binding energy of Co 2p<sub>3/2</sub> of Co<sup>0</sup> is higher than that of pure Co (777.9 eV). This is attributed to the difference in electron work function of Ni and Co.<sup>17</sup> Due to a lower electron work function, Co donates electron to Ni, leading to a shift of the binding energies of Ni and Co in Ni–Co alloy.<sup>11</sup> This also confirms the interaction of Ni with Co and formation of Ni–Co alloy, in consistence with the result of XRD analysis.

The above analysis results show that the interaction of Ni with Co and formation of Ni–Co alloy make the reduction of NiO easy in the reaction process and NiO–Co<sub>3</sub>O<sub>4</sub>/Nb<sub>2</sub>O<sub>5</sub>–TiO<sub>2</sub> catalyst can be completely reduced to Ni–Co/Nb<sub>2</sub>O<sub>5</sub>–TiO<sub>2</sub>. This result is consistent with that of H<sub>2</sub>–TPR, H<sub>2</sub>–TPD, XPS and XRD characterization in our previous study.<sup>10</sup> Furthermore, Ni/Co mass ratio has a great effect on the catalytic performance of NiO–Co<sub>3</sub>O<sub>4</sub>/Nb<sub>2</sub>O<sub>5</sub>–TiO<sub>2</sub> catalyst.

To analyze the reason for the best catalytic performance of the catalyst with a Ni/Co mass ratio of 8/3, number of d-band holes of NiO–Co<sub>3</sub>O<sub>4</sub>/Nb<sub>2</sub>O<sub>5</sub>–TiO<sub>2</sub> catalysts with different Ni/Co mass ratios is also listed in Table 3. The energy band theory links the electronic properties of a metal catalyst with its catalysis and d-band holes are used to describe state of valence electron of transition metals. There is a certain relationship among d-band holes of transition metals, adsorption strength of reaction component and the catalytic performance of the transition metal catalyst. Because of an existence of non-paired electrons, the transition metals can interact with reaction component to form chemical bonds. Only when the number of d-band holes in the metal is close to the number of electron transfer in the reaction, can the catalytic performance of the metal be better.<sup>18</sup> In hydrogenation reaction, the number of electron transfer of hydrogen molecule adsorbed on metal surface is 1, so the closer to 1 the number of d-band holes of metal catalyst is, the better the catalytic performance. It can be seen from Table 3 that number of d-band holes of the catalyst

**Table 3** Ni 2p and Co 2p XPS data of the recovered NiO–Co<sub>3</sub>O<sub>4</sub>/Nb<sub>2</sub>O<sub>5</sub>–TiO<sub>2</sub> with different Ni/Co mass ratios

Ni/Co	Binding energy/eV						Number of d-band holes		
	N <sup>0</sup>		Co <sup>0</sup>		Ni <sup>2+</sup>			Co <sup>2+</sup>	
	Ni 2p <sub>3/2</sub>	Co 2p <sub>3/2</sub>	Ni 2p <sub>3/2</sub>	Ni 2p <sub>1/2</sub>	Co 2p <sub>3/2</sub>	Co 2p <sub>1/2</sub>			
10	852.2	778.1	853.2	861.7	781.4	797.5	0.77		
8/3	852.1	778.2	855.7	872.9	781.0	797.0	0.99		
			853.8	861.9					
6/5	852.0	778.3	855.1	873.0	781.0	796.9	1.21		
			853.7	861.7					
4/7	852.0	778.3	855.7	873.3	781.0	796.9	1.43		
			853.8	862.2					
			855.8	873.2					





with a Ni/Co mass ratio of 8/3 is 0.99 (close to 1), so this catalyst should show an excellent catalytic performance, being consistent with the results of catalyst activity evaluation in Table 1.

### 3.2 Effect of NiO-Co<sub>3</sub>O<sub>4</sub> loading

The effect of NiO-Co<sub>3</sub>O<sub>4</sub> loading on catalytic performance of NiO-Co<sub>3</sub>O<sub>4</sub>/Nb<sub>2</sub>O<sub>5</sub>-TiO<sub>2</sub> with a Ni/Co mass ratio of 8/3 was investigated and the results are shown in Table 4. *n*-Valeraldehyde could be converted completely with an increase of the loading less than or equal to 17.5 wt%. However, conversion of *n*-valeraldehyde dropped to 88.0% over a NiO-Co<sub>3</sub>O<sub>4</sub>/Nb<sub>2</sub>O<sub>5</sub>-TiO<sub>2</sub> catalyst with a NiO-Co<sub>3</sub>O<sub>4</sub> loading of 21%, suggesting that the NiO-Co<sub>3</sub>O<sub>4</sub>/Nb<sub>2</sub>O<sub>5</sub>-TiO<sub>2</sub> catalyst with a NiO-Co<sub>3</sub>O<sub>4</sub> loading more than 17.5 wt% may not be reduced completely. The selectivity of 2-PH first increased, reached its highest value over the catalyst with a NiO-Co<sub>3</sub>O<sub>4</sub> loading of 14 wt%, then decreased and finally dropped to zero when NiO-Co<sub>3</sub>O<sub>4</sub> loading was 21 wt%. The selectivity of *n*-pentanol increased gradually and then decreased. When the loading was 10.5 wt%, the main product was 2-propylheptanal, indicating that the active component of hydrogenation was so less that 2-propylheptanal was not completely hydrogenated to 2-PH. When the loading was higher than 14 wt%, 2-propylheptanal or 2-propyl-2-heptenal was the main product, indicating that NiO and Co<sub>3</sub>O<sub>4</sub> were not completely reduced in reaction due to an over high loading, causing a lower hydrogenation activity.

The XRD patterns of NiO-Co<sub>3</sub>O<sub>4</sub>/Nb<sub>2</sub>O<sub>5</sub>-TiO<sub>2</sub> with different NiO-Co<sub>3</sub>O<sub>4</sub> loading before and after reaction are shown in

Table 5 Reusability of NiO-Co<sub>3</sub>O<sub>4</sub>/Nb<sub>2</sub>O<sub>5</sub>-TiO<sub>2</sub> catalyst<sup>a</sup>

Run	<i>X<sub>V</sub></i> /%	<i>S<sub>PO</sub></i> /%	<i>S<sub>2-PH</sub></i> /%
1	100	19.0	80.4
2	100	19.6	80.0
3	100	19.1	80.5
4	100	19.4	80.0
5	100	19.2	80.2

<sup>a</sup> Reaction conditions: a weight percentage of catalyst = 15%, *P* = 3 MPa, *T* = 200 °C, *t* = 5 h. V: *n*-valeraldehyde; PO: *n*-pentanol; 2-PH: 2-propylheptanol. X: conversion; S: selectivity.

Fig. 3. When the loading was less than or equal to 14 wt%, the diffraction peaks of NiO were not detected in the recovered catalysts, indicating that NiO could be completely reduced in reaction process. When the loading was higher than 14 wt%, the diffraction peaks of NiO could also be detected besides the diffraction peaks of metal Ni and Ni-Co alloy in the recovered catalysts, indicating that NiO could not be completely reduced in reaction process. The results are consistent with the results of catalyst activity evaluation in Table 4.

### 3.3 Reusability of NiO-Co<sub>3</sub>O<sub>4</sub>/Nb<sub>2</sub>O<sub>5</sub>-TiO<sub>2</sub> catalyst

The NiO-Co<sub>3</sub>O<sub>4</sub>/Nb<sub>2</sub>O<sub>5</sub>-TiO<sub>2</sub> catalyst with a Ni/Co mass ratio of 8/3 and a NiO-Co<sub>3</sub>O<sub>4</sub> loading of 14 wt% was used to evaluate the effect of reaction conditions (see Tables S1–S4 in the ESI<sup>†</sup>) and the suitable reaction conditions were determined as follows:

Table 4 Effect of NiO-Co<sub>3</sub>O<sub>4</sub> loading on catalytic performance of NiO-Co<sub>3</sub>O<sub>4</sub>/Nb<sub>2</sub>O<sub>5</sub>-TiO<sub>2</sub><sup>a</sup>

Loading of NiO and Co <sub>3</sub> O <sub>4</sub> /wt%	Loading of NiO/wt%	Loading of Co <sub>3</sub> O <sub>4</sub> /wt%	<i>X<sub>V</sub></i> /%	<i>S<sub>PO</sub></i> /%	<i>S<sub>2-PHEA</sub></i> /%	<i>S<sub>2-PHA</sub></i> /%	<i>S<sub>2-PH</sub></i> /%
10.5	7.5	3	100	13.4	0	73.2	12.4
14	10	4	100	18.2	0	0	81.4
17.5	12.5	5	100	23.7	0	45.5	28.9
21 <sup>b</sup>	15	6	88.0	5.2	75.6	18.1	0

<sup>a</sup> Reaction conditions: a weight percentage of catalyst = 15%, *T* = 200 °C, *P* = 3 MPa, *t* = 6 h. X: conversion; S: selectivity. V: *n*-valeraldehyde; PO: *n*-pentanol; 2-PHEA: 2-propyl-2-heptenal; 2-PHA: 2-propylheptanal; 2-PH: 2-propylheptanol. <sup>b</sup> The yield of *n*-pentanol, 2-propyl-2-heptenal, 2-propylheptanal and 2-propylheptanol was respectively 4.6%, 66.5%, 15.9% and 0%.

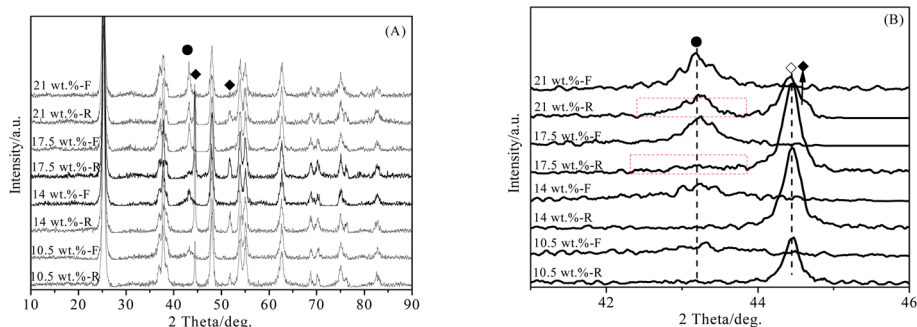


Fig. 3 XRD patterns of NiO-Co<sub>3</sub>O<sub>4</sub>/Nb<sub>2</sub>O<sub>5</sub>-TiO<sub>2</sub> with different NiO-Co<sub>3</sub>O<sub>4</sub> loading before and after reaction. F: fresh; R: recovered. ●: NiO; ◇: Ni-Co alloy; ◆: NiO. (A) XRD patterns; (B) enlarged view of XRD patterns.



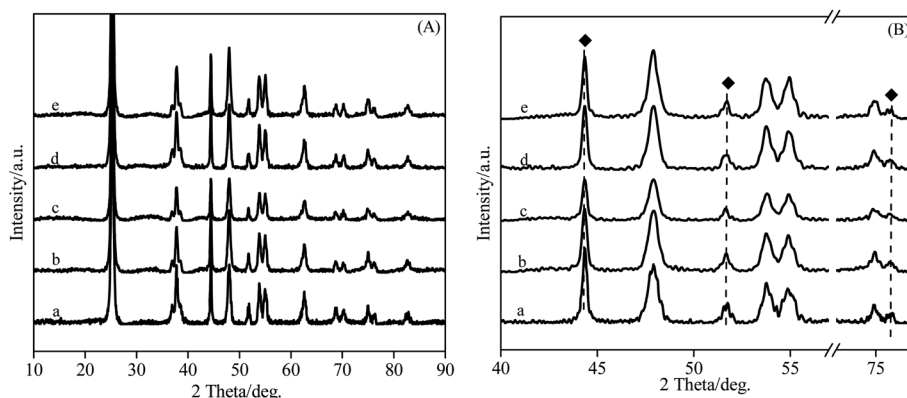


Fig. 4 XRD patterns of the recovered  $\text{NiO-Co}_3\text{O}_4/\text{Nb}_2\text{O}_5\text{-TiO}_2$ . (A) XRD patterns; (B) enlarged view of XRD patterns.  $\blacklozenge$ : Ni-Co alloy. (a) Recovered from 1<sup>st</sup> run (only drying); (b) recovered from 2<sup>nd</sup> run (only drying); (c) recovered from 3<sup>rd</sup> run (only drying); (d) recovered from 4<sup>th</sup> run (only drying); (e) recovered from 5<sup>th</sup> run (only drying).

a catalyst amount of 15 wt%, a reaction pressure of 3 MPa, a reaction temperature of 200 °C and a reaction time of 5 h. Under these conditions, the selectivity of 2-PH reached 80.4% at a *n*-valeraldehyde conversion of 100%.

The recovered  $\text{NiO-Co}_3\text{O}_4/\text{Nb}_2\text{O}_5\text{-TiO}_2$  catalyst was washed with ethanol, dried at 120 °C for 6 h, calcinated at 450 °C for 2 h and then was reused in the next cycle. The result of catalyst reusability is shown in Table 5. It can be seen that  $\text{NiO-Co}_3\text{O}_4/\text{Nb}_2\text{O}_5\text{-TiO}_2$  catalyst could be reused four times without a significant loss in its catalytic performance. Therefore,  $\text{NiO-Co}_3\text{O}_4/\text{Nb}_2\text{O}_5\text{-TiO}_2$  catalyst not only showed a high catalytic performance but also exhibited a good reusability.

The recovered  $\text{NiO-Co}_3\text{O}_4/\text{Nb}_2\text{O}_5\text{-TiO}_2$  catalyst was analyzed by means of XRD technique and the results are given in Fig. 4. According to literatures<sup>19,20</sup> and the PDF cards of JADE5.0 software, the peaks located at  $2\theta$  of 44.5°, 51.7° and 76.4° are attributed to pure metal Ni and the peaks located at  $2\theta$  of 44.3°, 51.5° and 75.9° are attributed to pure metal Co. It can be seen from Fig. 4 that the peaks located at  $2\theta$  of 44.4°, 51.6° and 76.2° can be detected in all the recovered catalysts without calcination (only dried).  $2\theta = 44.4^\circ$  of the corresponding (111) crystal facet is located at between 44.3° of pure metal Co (111) crystal facet and 44.5° of pure metal Ni (111) crystal facet, indicating that Ni-Co alloy phase is reserved during the reaction process. This result is in accordance with the XRD analysis in Fig. 2, suggesting that the Ni-Co alloy phase does not change with the reuse of catalyst.

Takanabe *et al.*<sup>21</sup> found that Co-Ni/TiO<sub>2</sub> catalyst with a Ni/Co ratio of 1 showed good catalytic activity and stability due to the formation of Ni-Co alloy. Similarly, Zhang *et al.*<sup>22,23</sup> used Ni-Me (Me = Co, Fe, Cu and Mn) bimetallic catalysts in carbon dioxide reforming of methane and found that Ni-Co bimetallic catalyst exhibited better activity and stability than other bimetallic catalysts due to the synergy between Ni and Co. From the above analysis, a good stability of  $\text{NiO-Co}_3\text{O}_4/\text{Nb}_2\text{O}_5\text{-TiO}_2$  should be attributed to the interaction of Ni with Co and formation of Ni-Co alloy in reaction process. Furthermore, both of them could be reserved stably in the process of reuse.

## 4. Conclusions

$\text{NiO-Co}_3\text{O}_4/\text{Nb}_2\text{O}_5\text{-TiO}_2$  catalyst can be completely reduced to Ni-Co/ $\text{Nb}_2\text{O}_5\text{-TiO}_2$  in reaction process. Its high catalytic performance is ascribed to the interaction of Ni with Co and formation of Ni-Co alloy. The  $\text{NiO-Co}_3\text{O}_4/\text{Nb}_2\text{O}_5\text{-TiO}_2$  catalyst with a Ni/Co mass ratio of 8/3 shows the best catalytic performance for its number of d-band holes is nearly equally to the number of electron transfer in hydrogenation reaction. The suitable  $\text{NiO-Co}_3\text{O}_4$  loading in  $\text{NiO-Co}_3\text{O}_4/\text{Nb}_2\text{O}_5\text{-TiO}_2$  catalyst is 14 wt%. Over high loading results in incomplete reduction of  $\text{NiO-Co}_3\text{O}_4$  and then a poor catalytic activity. The selectivity of 2-PH attains 80.4% with a complete conversion of *n*-valeraldehyde over the  $\text{NiO-Co}_3\text{O}_4/\text{Nb}_2\text{O}_5\text{-TiO}_2$  catalyst with a Ni/Co mass ratio of 8/3 and  $\text{NiO-Co}_3\text{O}_4$  loading of 14 wt%. Furthermore, the  $\text{NiO-Co}_3\text{O}_4/\text{Nb}_2\text{O}_5\text{-TiO}_2$  catalyst can be reused for four times without a decrease in its catalytic activity due to the reservation of the interaction of Ni with Co and formation of Ni-Co alloy.

## Conflicts of interest

There are no conflicts of interest to declare.

## Acknowledgements

This work was financially supported by National Natural Science Foundation of China (Grant No. 21476058, 21506046, 21978066) and Basic Research Program of Hebei Province for Natural Science Foundation and Key Basic Research Project (18964308D), and Natural Science Foundation of Hebei Province (B2018202220, B2020204023), and the Key Project for Natural Science Foundation of Hebei Province (B2020202048). The authors are gratefully appreciative of their contributions.

## References

- 1 S. K. Sharma and R. V. Jasra, *Indian J. Chem., Sect. A: Inorg., Bio-inorg., Phys., Theor. Anal. Chem.*, 2005, **54**, 451–458.

- 2 N. Liang, X. Zhang, H. An, X. Zhao and Y. Wang, *Green Chem.*, 2015, **17**, 2959–2972.
- 3 L. Kumaresan, A. Prabhu, M. Palanichamy and V. Murugesan, *Mater. Chem. Phys.*, 2011, **126**, 445–452.
- 4 L. Kumaresan, A. Prabhu, M. Palanichamy, E. Arumugam and V. Murugesan, *J. Hazard. Mater.*, 2011, **186**, 1183–1192.
- 5 A. Prabhu and M. Palanichamy, *Microporous Mesoporous Mater.*, 2013, **168**, 126–131.
- 6 A. Prabhu, A. Al Shoaibi, C. Srinivasakannan, M. Palanichamy and V. Murugesan, *J. Rare Earths*, 2013, **31**, 477–484.
- 7 L. Kumaresan, A. Prabhu, M. Palanichamy and V. Murugesan, *J. Taiwan Inst. Chem. Eng.*, 2010, **41**, 670–675.
- 8 L. Zhao, H. An, X. Zhao and Y. Wang, *Ind. Eng. Chem. Res.*, 2016, **55**, 12326–12333.
- 9 L. Zhao, One-step synthesis of 2-propyl heptanol from *n*-valeraldehyde, Doctoral thesis, Hebei University of Technology, Tianjin, People's Republic of China, 2019.
- 10 L. Zhao, H. An, X. Zhao and Y. Wang, *Catal. Commun.*, 2021, **149**, 106209.
- 11 L. Zhao, X. Mu, T. Liu and K. Fang, *Catal. Sci. Technol.*, 2018, **8**, 2066–2076.
- 12 P. Hu, Z. Y. Chen, T. Chang, J. Deng, F. Yang, K. Wang, Q. Li, B. Hu, H. Yu and W. Wang, *J. Alloys Compd.*, 2017, **727**, 332–337.
- 13 M. Madkour, Y. K. Abdel-Monem and F. Al Sagheer, *Ind. Eng. Chem. Res.*, 2016, **55**, 12733–12741.
- 14 J. Li, G. Lu, G. Wu, D. Mao, Y. Guo, Y. Wang and Y. Guo, *Catal. Sci. Technol.*, 2014, **4**, 1268–1275.
- 15 L. Xu, F. Wang, M. Chen, J. Zhang, K. Yuan, L. Wang, K. Wu, G. Xu and W. Chen, *ChemCatChem*, 2016, **8**, 2536–2548.
- 16 V. S. Kshirsagar, A. C. Garade, K. R. Patil, R. K. Jha and C. V. Rode, *Ind. Eng. Chem. Res.*, 2009, **48**, 9423–9427.
- 17 F. Yang, N. J. Libretto, M. R. Komarneni, W. Zhou, J. T. Miller, X. Zhu and D. E. Resasco, *ACS Catal.*, 2019, **9**, 7791–7800.
- 18 J. M. Huo, Carbon dioxide reforming of methane over Ni-Co bimetallic catalyst, *Master's thesis*, Taiyuan University of Technology, Shanxi, People's Republic of China, 2015.
- 19 A. W. Burns, A. F. Gaudette and M. E. Bussell, *J. Catal.*, 2008, **260**, 262–269.
- 20 W. Guo, W. Sun and Y. Wang, *ACS Nano*, 2015, **9**, 1462–11471.
- 21 K. Takanabe, K. Nagaoka, K. Nariai and K. Aika, *J. Catal.*, 2005, **232**, 268–275.
- 22 J. Zhang, H. Wang and A. K. Dalai, *J. Catal.*, 2007, **249**, 300–310.
- 23 J. Zhang, H. Wang and A. K. Dalai, *Appl. Catal., A*, 2008, **339**, 121–129.

